Conductance enhancement due to resonant tunneling into the subgap vortex core states in normal metal/superconductor ballistic junctions

M. A. Silaev
Institute for Physics of Microstructures, Russian Academy of Sciences, GSP-105, 603950 Nizhny Novgorod, Russia
(Received 11 September 2007; published 9 January 2008)

We investigate the low-energy quantum transport in ballistic normal metal-insulator-superconductor junction exposed to a magnetic field, creating Abrikosov vortices in the superconducting region. Within the Bogolubov–de Gennes theory, we show that the presence of the subgap quasiparticle states localized within the vortex cores near the junction interface leads to the strong resonant enhancement of Andreev reflection probability, and the normal-to-supercurrent conversion. The corresponding increase of charge conductance is determined by the distance from the vortex chain to the junction interface, which can be controlled by the applied magnetic field.

DOI: 10.1103/PhysRevB.77.014504 PACS number(s): 74.25.Fy, 74.25.Op, 73.40.Gk

I. INTRODUCTION

Recently, the investigation of transport properties of normal metal-superconducting (N/S) hybrid structures has attracted considerable interest. In the classical work by Blonder *et al.*,[1] it was shown that at the energies below the superconducting gap Δ_0, the charge transport can only be realized via the Andreev reflection at the N/S interface. This is a two-particle process in which the electrons with low energies $\varepsilon<\Delta_0$ incident from the normal metal (N) are reflected at the N/S interface as holes traversing the backward trajectories (and vice versa). In accordance with the charge conservation law, at the superconducting (S) region, the Cooper pairs are formed and the normal current converts into the supercurrent. For the perfectly transparent N/S interface, the charge doubling due to Andreev reflection results in enhancement of the subgap conductance by a factor of 2 compared with the corresponding normal state conductance. Being the two-particle process, Andreev reflection is strongly suppressed due to quasiparticle (QP) scattering at the layer of insulator separating the N and S regions. Indeed, in the case of the small interfactial barrier transparency $T\ll 1$, the Andreev reflection probability, and therefore the conductance, is proportional to T^2, which is smaller by a factor T as compared to the single-electron case.

The phenomenon of subgap conductance suppression results in the remarkable dependence of transport properties of N/S structures on the spatial distribution and symmetry of the superconducting gap. For example, recently, the charge current measurements were utilized for the direct observation of multivortex structures in mesoscopic superconductors.[2] The mixed state of mesoscopic superconductors is formed by a small number of vortices and reveals a rich variety of exotic vortex configurations, such as vortex molecules and multiquantum giant vortices, realized in such samples due to the quantum confinement of the Cooper pair motion.[3] In Ref. 2, the phase transitions between different vortex configurations were observed by the multiple-small-tunnel-junction method, in which several small tunnel junctions were attached to the mesoscopic superconductor to simultaneously measure the charge transport at the different points of the sample. The measured transport characteristics were related to the local density of states (DOS), depending on the local supercurrent density and, hence, on the configuration of the vortex system. Generally, when there is a uniform supercurrent flowing at the superconductor, the excitation spectrum acquires a Doppler shift by the value $\mathbf{v}_s\mathbf{p}_F$, where $\mathbf{v}_s$ is a superfluid velocity and $\mathbf{p}_F$ is a Fermi momentum. In this case, the minimal excitation energy is given by $E_{min}=\Delta_0-\mathbf{v}_s\mathbf{p}_F$. At large distances from the vortex core ($r\gg\xi$, where ξ is a coherence length), the Doppler shift model gives quite a good approximation of the QP spectrum with $v_s=\hbar/2mr$ (see Ref. 4). As long as the superfluid velocity is small compared to the critical value Δ_0/p_F, the Doppler shift of the gap edge results in the reduction of the height and broadening of the superconducting DOS peak.[5] Close to the vortex core ($r\sim\xi$) where $v_s\sim\Delta_0/p_F$, the gap edge E_{min} goes to zero. However, in this case, the Doppler shift model does not hold: it completely misses one of the remarkable features of the vortex state: the presence of low-energy QP states localized within the vortex core. These vortex core states were found in the pioneering work by Caroli–de Gennes–Matricon[6] (CdGM) within the more rigorous approach based on the quasiclassical solution of Bogoliubov–de Gennes (BdG) equations. It was shown that QP states with energy lower than the bulk superconducting gap value Δ_0 are localized within the vortex core and have the discrete spectrum ε_μ as a function of the quantized (half-integer) angular momentum μ. This spectrum of the CdGM states varies from Δ_0 to $-\Delta_0$ as μ changes from $-\infty$ to $+\infty$, crossing zero when μ changes its sign. At small energies $|\varepsilon|\ll\Delta_0$, the spectrum is given by $\varepsilon_\mu\approx-\mu\epsilon_0$, where $k_F=p_F/\hbar$ and $\epsilon_0=\Delta_0/k_F\xi$. For conventional superconductors, the interlevel spacing ϵ_0 is much less than the superconducting gap Δ_0 since $k_F\xi\gg 1$; therefore, the CdGM spectrum can be considered continuous as a function of the impact parameter of quasiclassical trajectory $b=-\mu/k_F$. The presence of the QP states bounded in the vortex core was confirmed in scanning tunnel spectroscopy (STS) experiments by the observation of the zero-bias conductance peak at the vortex core.[7] The analogous effect of the zero-bias conductance enhancement due to the resonant tunneling into the midgap surface states was thoroughly studied in high temperature D-wave superconductors.[8]

The goal of our work is to develop a theory to calculate the zero-bias conductance of N/S junction in the case when

the external magnetic field generates vortices in the S region near the N/S interface. We consider the charge transport across the direction of applied magnetic field. The N and S regions are assumed to be separated by the interfacial barrier, suppressing the Andreev reflection and the electron transport. We predict the strong enhancement of the Andreev reflection due to the resonant tunneling of QP through the barrier into the CdGM states localized within the vortex cores. The essential physics of this effect is analogous to the one which takes place in a double-barrier resonant tunneling diode.[9] The resonant tunneling in double-barrier quantum well structures occurs if the energy of incident QP wave coincides with the resonant energy, then the reflection probability is effectively suppressed due to the interference of the QP waves within the quantum well. In our case, the quantum well is represented by the vortex core and the bounded low-energy QP state consists of coupled electron and hole waves of almost the same amplitude. Therefore, if the incident electron has resonant energy, then the reflected electron wave is suppressed and the hole wave leaking from the vortex core contributes to the Andreev reflection probability. The important difference between our situation and the double-barrier diode case is that the spectrum of bound states is very dense, with the characteristic interlevel spacing $\epsilon_0 \sim \Delta_0/k_F\xi$ being much smaller than the bulk energy gap Δ_0. At the same time, the broadening of this level due to the finite barrier transparency can be estimated as $\delta E \sim \Delta_0 T e^{-2a/\xi}$, where T is the transparency of the interfacial barrier, the factor $e^{-2a/\xi}$ is due to the exponential decay of subgap QP at the superconducting slab of thickness a, which is, in fact, the distance from the vortex to the N/S interface, and ξ is the superconducting coherence length. Hereafter, in this paper, we will neglect the discreteness of the bound energy levels, assuming that $Te^{-2a/\xi} \geqslant (k_F\xi)^{-1}$. In fact, this condition is not very restrictive since $k_F\xi$ is large in many superconducting materials, for example, $k_F\xi \sim 3\times 10^2$ in Nb and $k_F\xi \sim 10^4$ in Al. Neglecting the discreteness of the spectrum of bounded QP states, we can use the quasiclassical approximation of QP quantum mechanics (see, e.g., Ref. 10). Within such approximation, QP moves along linear trajectories, i.e., the straight lines along the direction of QP momentum $\mathbf{n}=\mathbf{k_F}k_F^{-1}=(\cos\theta_p,\sin\theta_p)$. Note that for the N/S point contacts of atomic size in magnetic field, it is necessary to take into account the nonquasiclassical divergence of the electron and hole trajectories.[11] In the present work, we consider the transport properties of wide N/S junction so that its transverse dimension L_y is much larger than the Fermi wavelength $L_y \geqslant \lambda_F = 2\pi/k_F$; therefore, the trajectory divergence can be neglected. Also, we assume that L_y is much larger than the distance from the vortices to the N/S interface a and the characteristic intervortex distance L_v. The important point is that the total QP reflection probabilities can be found as a sum of individual vortex contributions. Indeed, the intervortex distance is much larger than the Fermi wavelength since $L_v \geqslant \xi$ and $k_F\xi \gg 1$. Therefore, the quasiclassical trajectories (except those with $\theta_p = \pm\pi/2$) can pass through not more than one vortex core. For some directions of QP momentum, two resonant trajectories (i.e., passing through the vortex cores) are coupled by the normal reflection at the interfacial barrier. Assuming the specularly reflecting barrier, this coupling occurs for the momentum angles at the narrow angle domains near $\theta_p = \arctan(nL_v/2a)$, where n is an integer. The width of the resonant angle domains $\delta\theta \sim Te^{-2a/\xi} \ll \pi$ is determined by the width of the resonant vortex core levels. Therefore, the contribution of such trajectories to the amplitude of the reflected QP waves, is negligible. Then, evaluating the amplitude of the QP wave we can separate the resonant trajectories coupled with bounded QP states localized within the different vortex cores. Since different trajectories do not interfere with each other, the resulting reflection probabilities and the conductance can be found as a sum of contributions from individual vortices.

The dimensionless conductance (further, we will measure it in terms of the conductance quantum $e^2/\pi\hbar$) induced by a single vortex at zero temperature can be estimated as follows: $G_v \sim N_r e^{-2a/\xi} T$. Here, $N_r \sim k_F\xi$ is the number of transverse modes of the N/S junction which effectively interact with the QP states bounded within the vortex core (ξ is the characteristic transverse size of the vortex core). The factor $e^{-2a/\xi}T$ is the one-particle tunneling probability through the barrier consisting of the insulating layer at the N/S interface and the superconducting slab of thickness a. The total vortex-induced conductance is the sum of the individual vortex contributions $G_{vt}=n_v G_v$, where $n_v = L_y/L_v$ is the total number of vortices near the N/S interface, L_v is the intervortex spacing, and L_y is the transverse size of the junction. The resonant mechanism of Andreev reflection exists along with the usual nonresonant scheme involving the two-particle tunneling through the interfacial barrier with the probability T^2. The corresponding zero-bias conductance can be estimated as $G_0 \sim N_0 T^2$, where $N_0 = k_F L_y/\pi$ is the total number of transverse modes in the N/S junction. Therefore, the total conductance of the N/S junction in magnetic field can be evaluated as follows:

$$G = \alpha N_0 T^2 + n_v \beta N_r e^{-2a/\xi} T, \tag{1}$$

where the coefficients $\alpha, \beta \sim 1$. Then, for the strong barrier $T \ll 1$, the conductance induced by the vortex chain with spacing L_v becomes dominant at $a < a_c$, where the threshold distance $a_c \sim (\xi/2)\ln(\xi/TL_v)$ can be much larger than the vortex core size and the coherence length.

The parameters of the vortex lattice can be estimated as follows: $a, L_v \sim \sqrt{\phi_0/B}$, where B is the average magnetic field of the superconducting sample and $\phi_0 = \pi\hbar c/e$ is the flux quantum. Then, the magnetic field dependence of the vortex-induced second term in Eq. (1) conductance is given by

$$G_{vt} \sim N_0 \sqrt{\frac{B}{H_{c2}}} e^{-2\sqrt{H_{c2}/B}} T, \tag{2}$$

where $H_{c2} \sim \phi_0/\xi^2$ is the upper critical magnetic field of the superconductor. Note that at zero magnetic field $B=0$, the conductance is $G \sim N_0 T^2$ and, at $B=H_{c2}$, the conductance is much larger: $G \sim N_0 T$. Therefore, we suggest that if the surface barrier is high $T \gg 1$, it should be possible to observe in experiment the field-induced increase of the conductance according to Eq. (2).

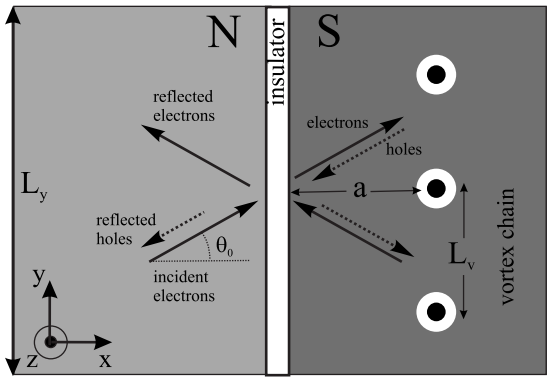

FIG. 1. Geometry of N/S junction and sketch of QP trajectories. The width of the junction is L_y. External magnetic field directed along the z axis introduces vortices in the superconductor. The distance from the first vortex chain to the N/S interface is a, and the intervortex spacing is L_v. The electrons are injected with the incident angle θ_0 and experience Andreev and normal reflections at the N/S interface.

In the present work, we do not take into account the subgap QP states which exists near the surface of superconductor due to the Meissner screening of external magnetic field.[12] Such QP levels lie higher at the energy scale than the CdGM states if the density of supercurrent near the surface is less than the critical value. Therefore, as long as the zero-bias conductance is considered, the influence of the surface QP states can be neglected.

The paper is organized as follows. In Sec. II, a description of the model and the basic equations are given. In Sec. III, we solve the scattering problem to find the Andreev and normal reflection probabilities. Section IV is devoted to the conductance calculation and Sec. V to the discussion of obtained results. Finally, conclusions are given in Sec. VI.

II. MODEL AND BASIC EQUATIONS

Shown in Fig. 1 is the scheme of the N/S junction with vortex lines in the S region parallel to the N/S interface. For the sake of simplicity, we assume that there is only one quantized QP mode in the z direction and take into account only the QP motion in the xy plane, perpendicular to the vortex lines.

Considering one vortex from the array, the coordinate system is chosen so that the z axis coincides with the vortex line, and the origin at the xy plane coincides with vortex phase singularity point. Neglecting the suppression of the superconductivity near the N/S interface due to the proximity effect, we assume that at $x > -a$ (superconducting region), the order parameter can be taken as follows:

$$\Delta(\mathbf{r}) = \Delta_0 D_v(\mathbf{r}) e^{i\Phi(\mathbf{r})}. \tag{3}$$

Here, Δ_0 is the gap value far from the vortex core, and $D_v(\mathbf{r})$ and $\Phi(\mathbf{r})$ are the dimensionless profile and the phase of the order parameter. The particular form of $D_v(\mathbf{r})$ is not essential for our consideration, therefore it can be chosen similar to the model profile of the isolated vortex core:[13] $D_v(\mathbf{r}) = r/\sqrt{r^2+\xi^2}$, where ξ is the coherence length. The phase distribution $\Phi(\mathbf{r})$ consists of a singular part $\Phi_v(\mathbf{r}) = \arg(\mathbf{r})$ and a regular part $\Phi_r(\mathbf{r})$, determined by the particular metastable vortex lattice configuration realized near the boundary.

In principle, the method developed in the present paper is applicable to the arbitrary order parameter phase distribution corresponding to the metastable vortex configuration. At first, we solve a generic problem of the influence of a single vortex near the N/S surface on the zero-bias conductance of the junction. The vortex stability condition given by the London model requires vanishing regular part of the superfluid velocity at the vortex position: $[\nabla\Phi_r - (2\pi/\phi_0)\mathbf{A}](\mathbf{r}=0) = 0$, where $\mathbf{A}$ is the vector potential. On the microscopic level, this condition is necessary for the existence of the CdGM QP states forming the vortex phase singularity.[14,15] The next step is the summation of the individual vortex contributions to the conductance, which add independently. The particular vortex configuration near the boundary depends on many factors, such as the random pinning potential, geometry of the superconducting sample, magnetization history, etc. To estimate the dependence of the conductance on the magnetic field, we consider the model situation assuming that the vortices near the boundary of the superconductor sit periodically on a chain with an intervortex spacing L_v at a distance a from the N/S interface. We take a and L_v as external parameters of the order a, $L_v \sim \sqrt{\phi_0/B}$, where B is the average magnetic field of the superconducting sample. The influence of the next vortex chains on the conductance can be neglected due to the rapid decay of the QP tunneling probability with the growing distance from vortices to the N/S interface.

The expression for the dimensionless zero-bias conductance of the N/S junction can be written as follows (see Ref. 1):

$$G = \frac{N_0}{2}\int_{-\pi/2}^{\pi/2} [1 - R_n(\theta_0) + R_a(\theta_0)]\cos\theta_0 d\theta_0, \tag{4}$$

where $R_n(\theta_0)$ and $R_a(\theta_0)$ are the probabilities of normal and Andreev reflections, respectively, and θ_0 is the incident angle: $\mathbf{k_F} = k_F(\cos\theta_0, \sin\theta_0)$. The total number of propagating modes N_0 is determined by the channel width: $N_0 = k_F L_y/\pi$. The problem of QP scattering at the N/S interface is formulated within the BdG theory. The equation for the electron and hole waves coupled by the superconducting gap $\Delta(\mathbf{r})$ reads as follows:

$$\begin{pmatrix} \hat{H}_0(\mathbf{r}) & \Delta(\mathbf{r}) \\ \Delta^*(\mathbf{r}) & -\hat{H}_0(\mathbf{r}) \end{pmatrix} \hat{\Psi}(\mathbf{r}) = E\hat{\Psi}(\mathbf{r}). \tag{5}$$

Here,

$$\hat{H}_0(\mathbf{r}) = \frac{1}{2m}\left(\hat{\mathbf{p}} - \frac{e}{c}\mathbf{A}\right)^2 - E_F + V(x),$$

with $\hat{\mathbf{p}} = -i\hbar\nabla$ and $\hat{\Psi}(\mathbf{r}) = (u(\mathbf{r}), v(\mathbf{r}))$. The interfacial barrier separating the N and S regions is modeled by the repulsive delta potential $V(x) = H\delta(x)$, parametrized by the dimensionless barrier strength $Z = H/\hbar V_F$.[1] The boundary conditions at the N/S interface are

$$[\hat{\Psi}(-a)]=0, \tag{6}$$

$$[\partial_x\hat{\Psi}(-a)]=(2k_FZ)\hat{\Psi}(-a), \tag{7}$$

where $[f(x)]=f(x+0)-f(x-0)$.

To overcome the complexity of the scattering problem coming from the broken spatial invariance of the superconducting gap, we treat Eq. (5) within quasiclassical approximation. Generally, the quasiclassical form of the wave function can be constructed as follows: $\hat{\Psi}(\mathbf{r})=e^{i\mathbf{k_F}\cdot\mathbf{r}}\hat{f}(\mathbf{r})$, where $\hat{f}(\mathbf{r})=(U(\mathbf{r}),V(\mathbf{r}))$ is a slowly varying envelope function. Then the system (5) reduces to the system of the first-order quasiclassical equations along the linear trajectories defined by the direction of the QP momentum $\mathbf{n}=\mathbf{k_F}k_F^{-1}=(\cos\theta_p,\sin\theta_p)$. Each trajectory is specified by the angle θ_p and the impact parameter $b=r\sin(\theta-\theta_p)$, where θ is the polar angle: $\mathbf{r}=-r(\cos\theta,\sin\theta)$. Introducing the coordinate along trajectory $s=(\mathbf{n}\cdot\mathbf{r})=-r\cos(\theta_p-\theta)$, we arrive at the following form of the quasiclassical equation: $\hat{H}\hat{f}=\epsilon\hat{f}$, with the Hamiltonian

$$\hat{H}=-i\xi\hat{\sigma}_z\partial_s+F+D_v(\hat{\sigma}_x\cos\Phi-\hat{\sigma}_y\sin\Phi), \tag{8}$$

where $\epsilon=E/\Delta_0,\xi=\hbar V_F/\Delta_0$ is the coherence length, $D_v(\mathbf{r})$ and $\Phi(\mathbf{r})$ are the dimensionless magnitude and phase of the order parameter, and $F(\mathbf{r})=(\pi\xi/\phi_0)\mathbf{n}\cdot\mathbf{A}$.

Considering the zero-bias problem, we will have to analyze only the zero-energy excitations with $\epsilon=0$. Within the normal metal region at $x<-a$, neglecting the influence of magnetic field on the QP motion, the quasiclassical equation (8) becomes trivial: $\partial_s\hat{f}(s,b)=0$. It means that the envelope function is constant along the trajectories.

Obviously, this is not the case at the superconducting region $x>-a$, where the electron and hole waves are coupled. Note that for the wave functions at the S region corresponding to the zero energy, the following representation can be used:[10] $\hat{f}=e^{\zeta}(e^{i(\eta+\Phi)/2},e^{-i(\eta+\Phi)/2})$, where $\zeta=\zeta(s,b)$ and $\eta=\eta(s,b)$ are real-valued functions. Then, the quasiclassical equation (8) can be written as follows:

$$\xi\partial_s\eta+2D_v\cos\eta+\epsilon_d=0, \tag{9}$$

$$\xi\partial_s\zeta+2D_v\sin\eta=0, \tag{10}$$

where $\epsilon_d(\mathbf{r})=\hbar\mathbf{k}_F\mathbf{v_s}/\Delta_0$ is the dimensionless Doppler shift energy. For the wave functions $\hat{f}_\pm$ decaying at the different ends of the trajectory $\hat{f}_\pm(s=\pm\infty)=0$ from Eq. (10), we obtain

$$\eta_\pm(s=\pm\infty)=\pm\pi/2. \tag{11}$$

As we will see below, the main contribution to the enhanced Andreev reflection probability comes from the trajectories with small impact parameters $|b|\ll\xi$, passing through the vortex core. For such trajectories, by neglecting the nonsingular part of the superfluid velocity near the vortex core, the analytical solution of Eq. (9) can be obtained following the results of Ref. 16:

$$\tan\eta_\pm=0.5(A_\pm^{-1}e^{-2K(s)}-A_\pm e^{2K(s)}), \tag{12}$$

$A_\pm=\gamma(b)[\mathrm{sgn}(s)\mp1]$, where $\gamma(b)=-\omega b$,

$$K(s)=\frac{1}{\xi}\int_0^s D_v(s')ds'=\sqrt{\left(\frac{s}{\xi}\right)^2+1}-1,$$

$$\omega=\frac{1}{\xi}\int_0^\infty\frac{D_v(s)}{s}e^{-2K(s)}ds.$$

III. SCATTERING PROBLEM: NORMAL AND ANDREEV REFLECTION PROBABILITIES

The boundary conditions (6) and (7) determine the specularly reflecting N/S interface, coupling the waves with wave vectors $\mathbf{k}_F=k_F(\cos\theta_0,\sin\theta_0)$, and $\mathbf{k}'_F=k_F(\cos(\pi-\theta_0),\sin(\pi-\theta_0))$. Therefore, if the incident electron wave is $u_i=e^{i\mathbf{k_F}\mathbf{r}}$, then reflected electron u_r and hole v_r waves will have the form

$$u_r=U_re^{i\mathbf{k}'_\mathbf{F}\mathbf{r}},\quad v_r=V_re^{i\mathbf{k_F}\mathbf{r}},$$

where $U_r(b,s)$ and $V_r(s,b)$ are the envelope functions. Each point $(-a,y)$ at the N/S interface lies on the intersection of two quasiclassical trajectories, characterized by the angles $\theta_p=\theta_0$ and $\theta_p=\pi-\theta_0$. From the simple trigonometry, it is easy to see that the impact parameters of these trajectories are $b_+=-a\sin(\theta_0-\theta)/\cos\theta$ and $b_-=-a\sin(\theta_0+\theta)/\cos\theta$, correspondingly, where $\theta=-\arctan(y/a)$ is the polar angle. The coordinate of the intersection point is $s_+=-a\cos(\theta-\theta_0)/\cos\theta$ and $s_-=a\cos(\theta+\theta_0)/\cos\theta$ for the trajectories characterized by the angles $\theta_p=\theta_0$ and $\theta_p=\pi-\theta_0$, correspondingly. Then, the reflection probabilities are given by

$$R_n(\theta_0)=\frac{a}{L_y}\int_{-\alpha}^{\alpha}|U_r(\theta,\theta_0)|^2(\cos\theta)^{-2}d\theta, \tag{13}$$

$$R_a(\theta_0)=\frac{a}{L_y}\int_{-\alpha}^{\alpha}|V_r(\theta,\theta_0)|^2(\cos\theta)^{-2}d\theta, \tag{14}$$

where the integration is done over the N/S interface, $\alpha=\arctan(L_y/2a),U_r(\theta,\theta_0)=U_r(b_-,s_-)$, and $V_r(\theta,\theta_0)=V_r(b_+,s_+)$.

Following the usual procedure to find the reflected wave amplitudes $U_r(\theta,\theta_0)$ and $V_r(\theta,\theta_0)$, one needs to match the N and S region solutions at the N/S interface. For the envelope functions, the boundary conditions (6) and (7) yield

$$1+U_r=e^{i\eta_+/2}C^+ + e^{i\eta_-/2}C^-,$$

$$V_r=e^{-i\eta_+/2}C^+ + e^{-i\eta_-/2}C^-,$$

$$(1-U_r)+2iZ(1+U_r)=e^{i\eta_+/2}C^+ - e^{i\eta_-/2}C^-,$$

$$V_r(1+2iZ)=e^{-i\eta_+/2}C^+ - e^{-i\eta_-/2}C^-,$$

C^+,C^- are arbitrary constants and $\eta_\pm=\eta_\pm(s_\pm,b_\pm)$, where $\eta_\pm(s,b)$ are the solutions of Eq. (9) with boundary conditions

(11) along the trajectories, with $\theta_p=\theta_0$ and $\theta_p=\pi-\theta_0$ for the upper and lower signs, correspondingly.

Solving this system, we obtain

$$U_r(\theta,\theta_0)=-\frac{(1-e^{i\chi})(\tilde{Z}^2-i\tilde{Z})}{1+\tilde{Z}^2(1-e^{i\chi})}, \tag{15}$$

$$V_r(\theta,\theta_0)=\frac{e^{-i\eta_+}}{1+\tilde{Z}^2(1-e^{i\chi})}, \tag{16}$$

where $\chi(\theta,\theta_0)=\eta_--\eta_+$ and $\tilde{Z}=Z/\cos\theta_0$.

Note that for the small impact parameters $|b_\pm|\ll\xi$, the factors $e^{i\eta_\pm}$ can be obtained analytically with the help of Eq. (12) as follows:

$$e^{i\eta_+}=i\frac{J-i(\theta-\theta_0)}{J+i(\theta-\theta_0)}, \tag{17}$$

$$e^{i\eta_-}=-i\frac{J-i(\theta+\theta_0)}{J+i(\theta+\theta_0)}, \tag{18}$$

where $J=e^{-2K(a/\cos\theta)}\cos\theta/2\omega a$. For the small angles $|\theta|,|\theta_0|\ll\xi/a$, Eqs. (17) and (18) are valid simultaneously, yielding

$$e^{i\chi}=-\frac{J^2+\theta^2-\theta_0^2-2i\theta_0 J}{J^2+\theta^2-\theta_0^2+2i\theta_0 J}. \tag{19}$$

IV. VORTEX-INDUCED ZERO-BIAS CONDUCTANCE

Now, using expressions (15) and (16) for the amplitudes of reflected waves and reflection probabilities (13) and (14), it is possible to find the zero-bias conductance. Introducing the function $g(\theta,\theta_0)=1-|U_r(\theta_0,\theta)|^2+|V_r(\theta_0,\theta)|^2$, the expression for the dimensionless conductance (4) reads as follows:

$$G=\frac{k_F a}{2\pi}\int_{-\alpha}^{\alpha}(\cos\theta)^{-2}d\theta\int_{-\pi/2}^{\pi/2}g(\theta,\theta_0)\cos\theta_0 d\theta_0, \tag{20}$$

where $\alpha=\arctan(L_y/2a)$. It is convenient also to introduce here a local conductivity, i.e., the conductance per unit length of the N/S surface:

$$\sigma(\theta)=\frac{k_F}{2\pi}\int_{-\pi/2}^{\pi/2}g(\theta,\theta_0)\cos\theta_0 d\theta_0.$$

Employing Eqs. (15) and (16), we obtain

$$g(\theta,\theta_0)=\frac{2}{(\tilde{Z}^4+\tilde{Z}^2)|1-e^{i\chi}|^2+1}. \tag{21}$$

If the applied magnetic field is zero and the superconductor is homogeneous $\chi=\pi$, we obtain $g(\theta,\theta_0)=g_0(\theta_0)$, where $g_0(\theta_0)=(1/2)(\tilde{Z}^2+1/2)^{-2}$. Then, the vortex-induced part of the conductivity is given by

$$\sigma_v(\theta)=\frac{k_F}{2\pi}\int_{-\pi/2}^{\pi/2}g_v(\theta,\theta_0)\cos\theta_0 d\theta_0,$$

where $g_v=g-g_0$:

$$g_v=\frac{(\tilde{Z}^4+\tilde{Z}^2)(4-|1-e^{i\chi}|^2)}{2(\tilde{Z}^2+1/2)^2[(\tilde{Z}^4+\tilde{Z}^2)|1-e^{i\chi}|^2+1]}.$$

To start the analysis of Eq. (21), let us note that for the low surface barrier $\tilde{Z}\to 0$, we get $g_v(\theta,\theta_0)=0$. In this case, all the incident QP undergo Andreev reflection and the zero-bias conductance is the same as in the case of a homogeneous superconductor: $G=2N_0$. As the barrier becomes higher, the Andreev reflection is suppressed and the conductance is reduced.

The function $g_v(\theta,\theta_0)$ reaches its maximum

$$g_{vm}=2\frac{\tilde{Z}^4+\tilde{Z}^2}{(\tilde{Z}^2+1/2)^2}$$

if $|1-e^{i\chi}|=0$. In fact, this condition determines the resonant trajectories corresponding to the zero-energy vortex core states modified by the normal reflection from the interfacial barrier. The resonant trajectories should pass through the vortex core, therefore the function $g_v(\theta,\theta_0)$ has a sharp peak at $\theta_0\approx\pm\theta$. The width of this peak is determined by the barrier strength and the distance from the vortex to the surface. For the small angles $|\theta|,|\theta_0|\ll\xi/a$, with the help of Eq. (19), we obtain

$$g_v(\theta_0,\theta)=\frac{g_{vm}J_0^2\theta_0^2}{(\tilde{Z}^2+1/2)^2(\theta_0^2-\theta^2-J_0^2)^2+J_0^2\theta_0^2}, \tag{22}$$

where $J_0=e^{-2K(a)}/2\omega a\sim(\xi/a)e^{-2a/\xi}$, which is a small parameter since $J_0\ll 1$ for $a\gtrsim\xi$. The maximum of $g_v(\theta,\theta_0)$ determined by Eq. (22) lies at $\theta_0^2=\theta^2+J_0^2$.

Employing Eq. (22), it is easy to compute the vortex-induced part of the conductivity $\sigma_v(\theta)$ at the small angle domain $|\theta|\ll\xi/a$. The main contribution to the integral over θ_0 comes from the small vicinity of the point $\theta_0=\theta$. Then with good accuracy, we obtain $\sigma_v=\sigma_{v0}$, where

$$\sigma_{v0}=k_F J_0\frac{Z^4+Z^2}{(Z^2+1/2)^3}. \tag{23}$$

At larger angles, the function $\sigma_v(\theta)$ can be evaluated only numerically. Numerical calculation described below shows that $\sigma_v(\theta)$ is maximal at $\theta=0$ and steadily decreases to zero as $|\theta|\to\pi/2$ (see inset in Fig. 2). Then, the resulting conductance induced by a single vortex $G_v=a\int_{-\alpha}^{\alpha}(\cos\theta)^{-2}\sigma_v(\theta)d\theta$ is given by

$$G_v=\beta(k_F\xi)e^{-2K(a)}\frac{Z^4+Z^2}{(Z^2+1/2)^3}, \tag{24}$$

where $\beta=(2\omega\xi)^{-1}\int_{-\alpha}^{\alpha}(\cos\theta)^{-2}\sigma_v(\theta)/\sigma_{v0}d\theta\sim 1$.

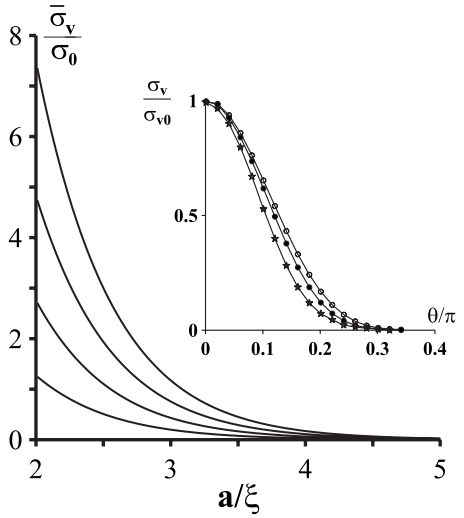

FIG. 2. Plot of the ratio $\bar{\sigma}_v/\sigma_0$ of the average vortex-induced conductivity to the conductivity in the absence of vortices. Curves from top to bottom correspond to $Z=5$, 4, 3, and 2. Inset: function $\sigma_v(\theta)/\sigma_{v0}$ for $a/\xi=2$ (open circles), $a/\xi=3$ (filled circles), and $a/\xi=5$ (asterisks); $Z=2$.

To evaluate the conductance rigorously, we find the factor $e^{i\chi}$ in Eq. (21) and then the reflection probabilities, solving numerically Eq. (9) with boundary conditions (11). We assume that the regular part of the phase distribution is $\Phi_r(\mathbf{r})=-\arg(\mathbf{r}-\mathbf{r}_{\mathbf{a}v})$ corresponding to the image vortex situated at the point $\mathbf{r}_{av}=(-2a,0,0)$ behind the N/S interface. The vector potential is chosen as $\mathbf{A}=B[\mathbf{z}_0\times(\mathbf{r}-\mathbf{r}_0)]/2$, where $\mathbf{r}_0=(-a,0,0)$ is the point at the boundary between the vortex and the image vortex, and $\mathbf{z}_0$ is the unit vector along the z axis. Within such model the condition of vanishing current through the N/S interface $[\partial_x\Phi-(2\pi/\phi_0)\mathbf{A}_x]=0$ is satisfied automatically, and the vortex stability is achieved by setting $a=\sqrt{\phi_0/B}$. The numerical plot of the function $\sigma_v(\theta)/\sigma_{v0}$ at different distances a from the vortex to the interface is presented in the inset in Fig. 2. The maximum value $\sigma_v(\theta=0)$ with good accuracy coincides with the analytical estimation given by Eq. (23). The coefficient β in Eq. (24) is found to be nearly constant as a function of a: it decreases slightly from $\beta\simeq 0.6$ at $a=2\xi$ to $\beta\simeq 0.4$ at $a=5\xi$. In Fig. 2, for the various magnitude of barrier strength, we plot the ratio $\bar{\sigma}_v/\sigma_0$ of the average vortex-induced conductivity $\bar{\sigma}_v=G_v/\xi$ to the conductivity of the N/S junction in the absence of vortices, given by

$$\sigma_0=\frac{k_F}{2\pi}\int_{-\pi/2}^{\pi/2} g_0(\theta,\theta_0)\cos\theta_0 d\theta_0.$$

V. DISCUSSION

Considering the strong barriers $Z\gg 1$, Eq. (24) can be written as $G_v=\beta(k_F\xi)e^{-2K(a)}T$, where we introduced the barrier transparency $T=(1+Z^2)^{-1}\approx Z^{-2}$. A simple understanding of this result can be obtained within the framework of the tunneling Hamiltonian approach.[17] The conventional expression for the tunneling conductivity of the N/S junction at zero temperature reads

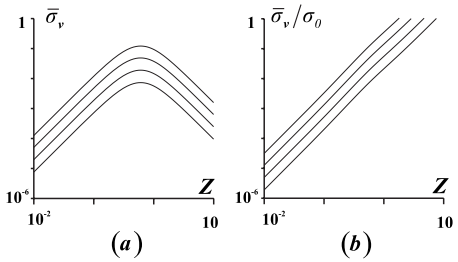

FIG. 3. (a) Plot of the average vortex-induced conductivity $\bar{\sigma}_v$ as a function of the barrier strength Z in logarithmic scale. (b) Plot of the ratio $\bar{\sigma}_v/\sigma_0$ as a function of the barrier strength Z in logarithmic scale. Curves from top to bottom correspond to $a/\xi=2$, 2.5, 3, and 3.5.

$$\sigma=\sigma_n\nu/\nu_0, \tag{25}$$

where ν is a local superconducting DOS at the Fermi level and σ_n is a normal state tunneling conductivity. For the S-wave superconductor, the transformation of vortex core states near the surface can be neglected at first approximation.[18] Then the local DOS near the surface at the Fermi level is determined by the density of vortex core states $\nu_v(\mathbf{r})$ given by[19,20]

$$\nu_v(\mathbf{r})=\frac{1}{2\pi}\int_0^{2\pi}|\hat{f}(\mathbf{r},\theta_p)|^2\delta[\epsilon_0 k_F r\sin(\theta-\theta_p)]d\theta_p, \tag{26}$$

where $\hat{f}(\mathbf{r},\theta_p)$ is the envelope of the QP wave function. For the CdGM wave functions $|\hat{f}(\mathbf{r},\theta_p)|^2\sim e^{-2K(r)}k_F/\xi$, then $\nu_v(\mathbf{r})\sim\nu_0(\xi/r)e^{-2K(r)}$, where $\nu_0=m/\hbar^2$ is the two-dimensional DOS at the normal metal. Substituting $\nu=\nu_v(r=a/\cos\theta)$ and $\sigma_n\sim Tk_F$, we obtain the conductivity $\sigma\sim k_F TJ(\theta)$, which coincides with the order of magnitude of expression (23) if $Z\gg 1$ and $|\theta|\ll 1$. Integrating $\sigma(\theta)$ over the N/S interface, we arrive at expression (24) for the conductance, with factor β given by $\beta\sim\int_{-\alpha}^{\alpha}\exp[2K(a)-2K(a/\cos\theta)](\cos\theta)^{-1}d\theta$. Note that although yielding the qualitatively right answer for the vortex-induced conductance, the tunneling Hamiltonian approach drops out the contribution from the nonresonant Andreev reflection with the probability of the order T^2. As we will see below, the contributions of the resonant and nonresonant Andreev reflections can be comparable even when the surface barrier is rather strong. Certainly, the tunneling Hamiltonian approach fails to provide the answer if the barrier strength is not very high, when the influence of vortices on the conductance is reduced, and the nonresonant Andreev reflection prevails. In Fig. 3(a), we show in logarithmic scale the vortex-induced conductivity $\bar{\sigma}_v$ as a function of the barrier strength Z for several values of the distance a. At small values of Z, the function $\bar{\sigma}_v(Z)$ grows $\bar{\sigma}_v\sim Z^2$ in accordance with the estimation (23). At larger values of the barrier strength $Z\gg 1$, the behavior of $\bar{\sigma}_v(Z)$ changes to $\bar{\sigma}_v\sim Z^{-2}$, but, at the same time, the conductivity without vortices at $Z\gg 1$ behaves as σ_0

$\sim Z^{-4}$. Therefore, the ratio $\bar{\sigma}_v/\sigma_0$ is monotonically growing as a function of the barrier strength Z proportional to Z^2 [see Fig. 3(b)].

Let us have a look at the expression for the total conductance of the N/S junction, which has quite a simple form if $Z \gg 1$. Neglecting edge effects and summing up the individual vortex contributions, we obtain

$$G = (8/15)N_0T^2 + n_v\beta(k_F\xi)e^{-2K(a)}T, \tag{27}$$

where $n_v = L_y/L_v$ is the total number of vortices near the N/S interface. The obtained expression for the total conductance (27) consists of two terms. The first term $G_0 \sim N_0T^2$ coincides with the conductance of the N/S junction at zero magnetic field. The factor T^2 is determined by the probability of the sequential tunneling of the incident and reflected QP through the high interfacial barrier. The second term is the total vortex-induced conductance $G_{vt} = n_vG_v \sim n_v(k_F\xi)e^{-2K(a)}T$; it comes from the tunneling of the incident QP into the zero-energy CdGM states inside the vortex core. Indeed, it is easy to see that $e^{-2K(a)}T$, where $K(a) = \sqrt{(a/\xi)^2+1}-1$, is the one-particle tunneling probability through the interfacial barrier and the superconducting layer of thickness a with slightly suppressed gap due to the presence of the vortex. The factor $k_F\xi$ is the number of resonant transverse modes for a single vortex. The vortex-induced conductance G_{vt} prevails over G_0 when $a < a_c$, where the critical distance a_c is determined by $a_c \approx (\xi/2)\ln(L_v/T\xi)$. The parameters of the vortex configuration, such as the intervortex spacing L_v and the distance a from the vortex array to the boundary of superconductor, are determined by the magnetic field; therefore, the conductance of the N/S junction can be controlled by the magnetic field. Using Eq. (2), we obtain that the critical magnetic field B_c when $G_{vt} \sim G_0$ is determined by the following transcendental equation: $\ln(x/T) = 2/x$, where $x = \sqrt{B/H_{c2}}$. Taking, for example, the barrier strength $Z=5$, we obtain that the critical field is $B_c \sim 0.5H_{c2}$ and the critical distance $a_c \sim 1.5\xi$. Therefore, the influence of the resonant vortex core states on the conductance can become significant when the magnetic field is less than the upper critical field and vortices are quite far from the N/S interface.

Finally, we should note that in real N/S junctions, the motion of QP is certainly affected by impurity scattering. The influence of impurities can be neglected completely, assuming that the lifetime of the vortex core states due to the finite barrier transparency is much shorter than the relaxation time of the QP momentum: $\hbar/\delta E \ll \tau$, or

$$l_e \gg (Te^{-2a/\xi})^{-1}\xi, \tag{28}$$

where $l_e = V_F\tau$ is an elastic mean free path of QP at the S region. This condition certainly can be fulfilled if the barrier transparency is not very high, i.e., $T \sim 1$, and the vortex chain is situated not far from the N/S interface, so that the factor $Te^{-2a/\xi}$ is not very small. Otherwise, if condition (28) is not fulfilled, the impurity scattering will modify the conductance. The simplest approach to estimate the conductance in this situation is based on the tunneling Hamiltonian, yielding Eq. (25) for the conductivity. Due to the impurity scattering, the local superconducting DOS differs from that given by Eq. (26), which is valid for the clean case $l_e \gg \xi$. In particular, the sharp peak at $r=0$ is smeared; therefore, at the center of the vortex, the DOS is smaller as compared to the clean case. However, at distances $r > \xi$ from the vortex core (e.g., at the N/S interface), the DOS is not suppressed by the impurities even if $l_e \sim \xi$. On the contrary, it is even larger than in the clean case due to the smearing of the DOS peak at the center of the vortex.[21] Therefore, in the case of the rather high impurity concentration on the S side, the dependence of the vortex-induced conductance on the magnetic field is still described by Eq. (2). Another important point is the influence of impurities on the nonresonant part of the conductance, i.e., the first term in Eq. (1). In particular, the interference of QP waves reflected from the interface barrier and impurities on the N side of the N/S junction can also result in the low-bias conductance enhancement, known as reflectionless tunneling (see Ref. 22 and references therein). In experiments where the reflectionless tunneling effect was observed,[24] the condition $l_e > \xi$ was fulfilled. In this case, the critical value of magnetic field suppressing the reflectionless tunneling[23] $H_c \sim \phi_0/12l_e^2$ was much less than the upper critical field of the superconductor. In our case, the applied magnetic field must be strong enough to create the dense vortex lattice in the superconductor: $B \sim H_{c2} \gg H_c$. Therefore, under the same experimental conditions as in Ref. 24, the reflectionless tunneling effect is absent in the range of magnetic fields that we are interested in.

VI. CONCLUSION

To summarize, we have investigated the low-energy charge transport in N/S junction across the direction of applied magnetic field. We have found the strong enhancement of the zero-bias conductance due to the resonant tunneling of the incident QP into the subgap vortex core states. The effect is most sound if the conventional channel of Andreev reflection is suppressed by the high interfactial barrier. Note that, usually, the vortex core states are investigated in STS experiments, where the charge transport is measured along the direction of magnetic field. For an alternative to the STS methods, now we can suggest the transport measurements in planar structure with wide-area N/S contacts. The vortex-induced conductance that we have studied depends exponentially on the distance from the vortex chain to the N/S interface and, therefore, can be effectively controlled by the external magnetic field. Also, for the possible experimental setup, one can consider the mesoscopic superconducting sample with lateral tunneling junctions, such as in Ref. 2. Since the vortex-induced conductance is proportional to the number of vortices, the conductance vs magnetic field dependence should reveal pronounced steps marking the switch of the total vorticity of the sample.

ACKNOWLEDGMENTS

It is my pleasure to thank Alexander S. Mel'nikov for numerous stimulating discussions and help in preparation of this paper. Also I am grateful to Ekaterina Ezhova for help with numeric calculations and to A. A. Andronov, V. V. Kurin, S. V. Sharov, D. Vodolazov, and D. Ryzhov for useful discussions. This work was supported, in part, by Russian Foundation for Basic Research, by Program "Quantum Macrophysics" of RAS, and by Russian Science Support and "Dynasty" Foundations.

[1] G. E. Blonder, M. Tinkham, and T. M. Klapwijk, Phys. Rev. B **25**, 4515 (1982).

[2] A. Kanda, B. J. Baelus, F. M. Peeters, K. Kadowaki, and Y. Ootuka, Phys. Rev. Lett. **93**, 257002 (2004); B. J. Baelus, A. Kanda, F. M. Peeters, Y. Ootuka, and K. Kadowaki, Phys. Rev. B **71**, 140502(R) (2005); B. J. Baelus, A. Kanda, N. Shimizu, K. Tadano, Y. Ootuka, K. Kadowaki, and F. M. Peeters, *ibid.* **73**, 024514 (2006).

[3] G. Boato, G. Gallinaro, and C. Rizzuto, Solid State Commun. **3**, 173 (1965); D. S. McLachlan, *ibid.* **8**, 1589 (1970); V. A. Schweigert, F. M. Peeters, and P. S. Deo, Phys. Rev. Lett. **81**, 2783 (1998); A. K. Geim, S. V. Dubonos, J. J. Palacios, I. V. Grigorieva, M. Henini, and J. J. Schermer, *ibid.* **85**, 1528 (2000); L. F. Chibotaru, A. Ceulemans, V. Bruyndoncx, and V. V. Moshchalkov, Nature (London) **408**, 833 (2000); A. K. Geim, S. V. Dubonos, J. J. Palacios, I. V. Grigorieva, M. Henini, and J. J. Schermer, Phys. Rev. Lett. **85**, 1528 (2000).

[4] M. Tinkham, *Introduction to Superconductivity*, 2nd ed. (McGraw-Hill, New York, 1996), Chap. 10.

[5] A. Anthore, H. Pothier, and D. Esteve, Phys. Rev. Lett. **90**, 127001 (2003).

[6] C. Caroli, P. G. de Gennes, and J. Matricon, Phys. Lett. **9**, 307 (1964).

[7] H. F. Hess, R. B. Robinson, R. C. Dynes, J. M. Valles, Jr., and J. V. Waszczak, Phys. Rev. Lett. **62**, 214 (1989); H. F. Hess, R. B. Robinson, and J. V. Waszczak, *ibid.* **64**, 2711 (1990); A. Kohen, Th. Proslier, T. Cren, Y. Noat, W. Sacks, H. Berger, and D. Roditchev, *ibid.* **97**, 027001 (2006).

[8] C. R. Hu, Phys. Rev. Lett. **72**, 1526 (1994); J. Yang and C. R. Hu, Phys. Rev. B **50**, 16766 (1994); Y. Tanaka and S. Kashiwaya, Phys. Rev. Lett. **74**, 3451 (1995); S. Kashiwaya, Y. Tanaka, M. Koyanagi, H. Takashima, and K. Kajimura, Phys. Rev. B **51**, 1350 (1995).

[9] B. Ricco and M. Ya. Azbel, Phys. Rev. B **29**, 1970 (1984).

[10] J. Bardeen, R. Kummel, A. E. Jacobs, and L. Tewordt, Phys. Rev. **187**, 556 (1969).

[11] N. B. Kopnin, A. S. Melnikov, and V. M. Vinokur, Phys. Rev. B **71**, 052505 (2005).

[12] P. Pincus, Phys. Rev. **158**, 346 (1967).

[13] J. R. Clem, J. Low Temp. Phys. **18**, 427 (1975).

[14] G. E. Volovik, Pis'ma Zh. Eksp. Teor. Fiz. **58**, 444 (1993) [JETP Lett. **58**, 455 (1993)].

[15] F. Gygi and M. Schluter, Phys. Rev. B **43**, 7609 (1991).

[16] N. B. Kopnin, A. S. Mel'nikov, and V. M. Vinokur, Phys. Rev. B **68**, 054528 (2003).

[17] G. D. Mahan, *Many-Particle Physics*, 2nd ed. (Plenum, New York, 1993), Chap. 9.

[18] S. Graser, C. Iniotakis, T. Dahm, and N. Schopohl, Phys. Rev. Lett. **93**, 247001 (2004).

[19] N. Schopohl and K. Maki, Phys. Rev. B **52**, 490 (1995).

[20] N. B. Kopnin and G. E. Volovik, JETP Lett. **64**, 690 (1996).

[21] P. Miranovic, M. Ichioka, and K. Machida, Phys. Rev. B **70**, 104510 (2004).

[22] C. W. J. Beenakker, Rev. Mod. Phys. **69**, 731 (1997).

[23] B. J. van Wees, P. de Vries, P. Magnee, and T. M. Klapwijk, Phys. Rev. Lett. **69**, 510 (1992).

[24] A. Kastalsky, A. W. Kleinsasser, L. H. Greene, R. Bhat, F. P. Milliken, and J. P. Harbison, Phys. Rev. Lett. **67**, 3026 (1991).